analytical chemistry

Subscriber access provided by MONASH UNIVERSITY

Article

Electrochemical Label-Free Aptasensor for Specific Analysis of Dopamine in Serum in the Presence of Structurally Related Neurotransmitters

Isabel Álvarez-Martos, and Elena E Ferapontova

Anal. Chem., **Just Accepted Manuscript** • DOI: 10.1021/acs.analchem.5b04207 • Publication Date (Web): 26 Feb 2016

Downloaded from http://pubs.acs.org on February 27, 2016

Just Accepted

"Just Accepted" manuscripts have been peer-reviewed and accepted for publication. They are posted online prior to technical editing, formatting for publication and author proofing. The American Chemical Society provides "Just Accepted" as a free service to the research community to expedite the dissemination of scientific material as soon as possible after acceptance. "Just Accepted" manuscripts appear in full in PDF format accompanied by an HTML abstract. "Just Accepted" manuscripts have been fully peer reviewed, but should not be considered the official version of record. They are accessible to all readers and citable by the Digital Object Identifier (DOI®). "Just Accepted" is an optional service offered to authors. Therefore, the "Just Accepted" Web site may not include all articles that will be published in the journal. After a manuscript is technically edited and formatted, it will be removed from the "Just Accepted" Web site and published as an ASAP article. Note that technical editing may introduce minor changes to the manuscript text and/or graphics which could affect content, and all legal disclaimers and ethical guidelines that apply to the journal pertain. ACS cannot be held responsible for errors or consequences arising from the use of information contained in these "Just Accepted" manuscripts.

ACS Publications

Analytical Chemistry is published by the American Chemical Society. 1155 Sixteenth Street N.W., Washington, DC 20036

Published by American Chemical Society. Copyright © American Chemical Society. However, no copyright claim is made to original U.S. Government works, or works produced by employees of any Commonwealth realm Crown government in the course of their duties.

Electrochemical Label-Free Aptasensor for Specific Analysis of Dopamine in Serum in the Presence of Structurally Related Neurotransmitters

Isabel Álvarez-Martos[a,b] and Elena E. Ferapontova[a,b]*

[a] *Interdisciplinary Nanoscience Center (iNANO) and* [b]*Danish National Research Foundation: Center for DNA Nanotechnology (CDNA), Aarhus University, Gustav Wieds Vej 1590-14, DK-8000 Aarhus C, Denmark*

* e-mail: elena.ferapontova@inano.au.dk, tel. +45 8715 6703

Abstract: Cellular and brain metabolism of dopamine can be correlated with a number of neurodegenerative disorders, and as such *in vivo* analysis of dopamine in the presence of structurally related neurotransmitters (NT) represents a Holy Grail of Neuroscience. Interference from those NTs generally does not allow selective electroanalysis of dopamine, which redox transformation overlaps with those of other catecholamines. In our previous work we reported an electrochemical RNA-aptamer based biosensor for specific analysis of dopamine (Analytical Chemistry 85 (2013) 121). However, the overall design of the biosensor restricted its stability and impeded its operation in serum. Here, we show that specific biorecognition and electroanalysis of dopamine in serum can be performed by the RNA aptamer, tethered to cysteamine-modified gold electrodes via the alkanethiol linker. The stabilized dopamine aptasensor allowed continuous 20 h amperometric analysis of dopamine in 10% serum, within the physiologically important 0.1—1 μM range and in the presence of catechol and such dopamine precursors and metabolites as norepinephrine and L-DOPA. In a flow-injection mode, the aptasensor response to dopamine was ~ 1 s, the sensitivity of analysis, optimized by adjusting the aptamer surface coverage, was 67 ± 1 nA μM^{-1} cm^{-2}, and the dopamine LOD was 62 nM. The proposed design of the aptasensor, exploiting both the aptamer alkanethiol tethering to the electrode and screening of the catecholamine-aptamer electrostatic interactions, allows direct monitoring of dopamine levels in biological fluids in the presence of competitive NT, and thus may be further applicable in biomedical research.

Keywords. Dopamine, RNA aptamer, electrochemical aptasensor, gold electrodes, electroanalysis

INTRODUCTION

Such dysfunctions of the human brain as depression, alcohol and drug addiction, and such neurological disorders as Parkinson's disease (PD) and schizophrenia, are associated with abnormalities in neurotransmitter (NT) metabolism in brain, and account for 35% of the disease burden in the Western World.[1] In particular, dopamine is a NT that plays a major role in cognition, motivation/learning, sleep, attention and regulation of movement, and is implicated in the pathophysiology of PD, psychosis and drug addiction.[2] Thus, it is considered as an important biomarker for mechanistic studies of behavior and diseases, their diagnosis, therapy and prognosis, which directly depend on the possibility of specific real-time analysis of dopamine, being a Holy Grail of Neuroscience indeed.

Several methods have been developed for *in vivo* monitoring of dopamine at its physiological relevant levels (in human serum/blood plasma ranged between the basal 1 nM level[3] and 0.9 – 6 μM found in L-dopa treated Parkinson's patients[4]; and in the brain varied between basal 10 nM and 1 μM reached during the dopamine release)[5]: carbon fiber microelectrodes, microdialysis, positron emission tomography (PET) scanning, and fluorescence spectroscopy. Microdialysis sampling method combined with a powerful separation technique (e.g. high-performance liquid chromatography or capillary/microchip electrophoresis) has proven to be a versatile and successful method for monitoring dopamine in the extracelular fluid of the brain.[6,7] However, many neurochemical events, such as dopamine release and its further transformation, occur at the time-scale of a few seconds or less, and thus NT concentration variations could be misestimated due to the limited temporal resolution of this technique (time scale of minutes). Dopamine fluctuations are best measured by tools with greater temporal precision, such as fast-scan cyclic voltammetry (FSCV) or constant potential amperometry;[8] both electrochemical techniques allow detection of dopamine on a time-scale of milliseconds. Moreover, the use of carbon fiber microelectrodes (~ 10 μm in diameter) provides a high spatial precision of dopamine detection, with a resolution exceeding that microdialysis probes. [9,10]

Indeed, electrochemical approaches have been extensively employed for dopamine analysis in biological systems,[11-14] rats,[15] drosophila flies,[16] brain slices,[17] and cells.[18] Various electrode materials and modifications (e.g. self-assembled monolayers, permselective membranes, metal nanoparticles and oxides, carbon nanomaterials and polymers) have been tested.[19] However the major problem of their use in biological systems containing electrochemically interfering NTs,

sharing the same catechol group as dopamine and whose electrochemical "signatures" are similar to those of dopamine, remains the same.[20] While interference from ascorbic acid (AA) and uric acid (UA) can be avoided by proper modification of electrodes,[19] inference from structurally related catecholamines is difficult to overcome, and it requires selectivity of biological reactions provided for example by dopamine receptors[21] or wisely used (otherwise nonspecific for dopamine) enzymatic systems.[22,23]

We have recently reported an electrochemical label-free RNA aptamer-modified electrode for sensitive and specific biorecognition of dopamine in the presence of structurally related NTs.[24] Aptamers are either DNA or RNA sequences selected *in vitro* that can with high affinity and specificity recognize and bind certain ligands, from small molecules to cells and tissues, and they are widely used in electrochemical biosensor schemes.[25] In our previous work, the RNA aptamer capable of specific 1:1 binding of dopamine,[26] was immobilized onto a cysteamine-modified gold electrode via electrostatic interactions, which allowed both its immobilization and retaining the conformational freedom and binding affinity towards dopamine. This RNA aptamer sequence, with its dopamine-binding site composed of two stem-loop domains trapping dopamine in (in each loop a region of five nucleotides being involved in dopamine biorecognition), has been proven to possess a high affinity for dopamine.[26] Most important, the positively charged cysteamine self-assembled monolayer (SAM) screened the negative charges on the aptamer, which provided the selectivity of dopamine binding higher that that shown in solution.[24] The apparent affinity of the aptamer for dopamine became superior to that shown in solution (reflected in the decreased apparent dissociation constant of 0.12±0.01 μM versus 1.6±0.17 μM, correspondingly).[27] Dopamine binding by the aptamer strongly depended on the aptamer surface coverage, and under optimal experimental conditions 0.1-2 μM dopamine could be specifically detected with a 85.4 nA μM^{-1} cm^{-2} sensitivity sufficient for practical applications.[27]

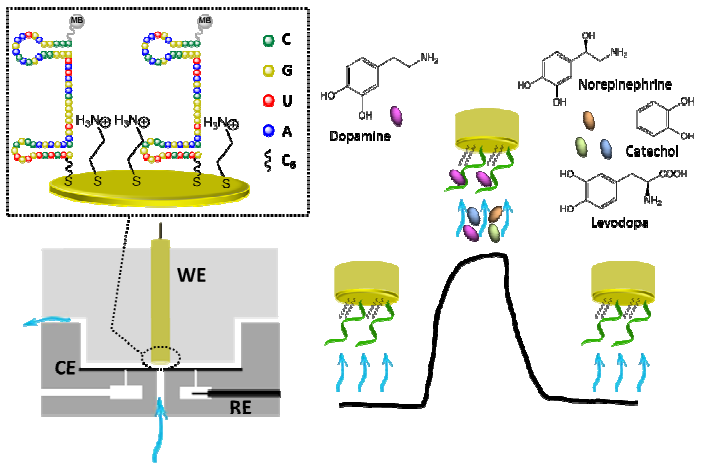

Figure 1. Schematic representation of (left panel) the flow-through wall-jet electrochemical cell (with working electrode, WE, counter electrode, CE, and an $Ag/AgCl_{(0.1\ M\ KCl)}$ reference electrode, RE) used for dopamine electroanalysis and the aptamer-modified gold electrode surface. The right panel image shows the chronoamperometric response of the aptasensor to dopamine, selectively trapped from the flow of NTs over the sensor surface. After each measurement the electrode surface was regenerated in a flow of a blank buffer solution, to remove the oxidized analyte.

However, in these pioneer works demonstrating the principal applicability of the aptasensor for specific analysis of dopamine**,** insufficient stability of electrostatic binding of the aptamer to the modified electrodes excluded practical analysis of dopamine either in biological fluids (serum) or during experiments that require prolonged measurements such as in behaving animals: a quite fast, after just a few cycles of measurements/regeneration, removal of the electrostatically bound aptamer from the electrode surface did occur.[24]

Here, we report a specific, sensitive and more stable electrochemical aptasensor that can operate in serum and thus is suitable for *in vivo* monitoring of dopamine. In this design, the aptamer was immobilized on the electrode via an alkanethiol C6 linker. Several issues were to be addressed: (i) Co-adsorption of the thiolated aptamer and cysteamine SAM that should compensate the negative charge of the aptamer and by this prevent non-specific electrostatic interactions between the aptamer and catecholamines; thermodynamically, the aptamer C6 alkanethiol stronger binds to gold and might replace C2 cysteamine, while shorter linkers might not provide desirable stability of the aptamer binding; (ii) Stronger binding of the C6-thiolated aptamer to gold might result in a too high surface coverage of the aptamer, providing steric restrictions for dopamine binding; (iii) If stability of the aptamer in serum (against digestion by nucleases) would be sufficient for the aptasensor operation. Previously, we used specially treated serum solutions for electroanalysis with RNA aptamers;[28,29] such treatment is excluded for any *in vivo* applications; (iv) Since it is solely the reduced form of dopamine that the aptamer selectively recognizes, can the aptasensor be

regenerated by dopamine oxidation? And, finally, (v) What is the time-scale of the dopamine-aptamer binding, is it sufficiently fast for real-time monitoring of dopamine? If those issues would be addressed, the developed aptasensor could then contribute to *in vivo* electroanalysis of neurodegenerative diseases, assisting in revealing e.g. the pathways and mechanisms of amyloidosis in brain [30,31] for which electroanalytical sensing platforms are currently being developed,[32-35] and to *in vitro* screening of drug-administered Parkinson's patients.[4]

EXPERIMENTAL

Materials. NTs, buffer solution components, cysteamine, tris(2-carboxyethyl)phosphine hydrochloride (TCEP) and ethanol (EtOH, ≥99.8%) were from Sigma-Aldrich (Germany). All chemicals were of the analytical grade and used as received. The 57-mer 5′-thiol-C_6-modified RNA aptamer specific for dopamine (HO-C6-S-S-C6-5′-GUC UCU GUG UGC GCC AGA GAC AGU GGG GCA GAU AUG GGC CAG CAC AGA AUG AGG CCC-3′)[26] was synthesized by MetaBion (Germany). The MB-labeled aptamer was prepared as previously described[36] by conjugation of 5′-amino-C_6-modified RNA (HO-C6-S-S-C6-5′-GUC UCU GUG UGC GCC AGA GAC AGU GGG GCA GAU AUG GGC CAG CAC AGA AUG AGG CCC-3′-NH_2) aptamer obtained from RiboTask (Denmark) with succinimide esther activated methylene blue (empBiotech, Berlin, Germany). Water was purified by a Milli-Q system (18 MΩ, Millipore, Bedford, MA, USA). Stock solutions of catecholamines were daily prepared in 20 mM phosphate buffer solution containing 0.15 M NaCl (PBS), pH 7.4, and protected from light.

Electrodes cleaning and surface area determination. Polycrystalline gold disk electrodes (0.2 cm in diameter, CH Instruments, Austin, TX) were electrochemically cleaned in 0.5 M NaOH by potential cycling between -0.5 and -1.4 V, then polished to a mirror luster in 1 μm diamond and 0.1 μm alumina slurries (Struers, Denmark) on microcloth pads (Buehler, Germany) and ultrasonicated for 15 min in the 1:1 EtOH/water mixture. Finally, the electrodes were electrochemically polished in 1 M H_2SO_4 and 0.5 M H_2SO_4/10 mM KCl by cycling between 0 and 1.7 V. The electrochemically active electrode surface area was determined from the reduction peak of gold surface oxide, assuming a 400 μC cm^{-2} required for the reduction of a monolayer of chemisorbed oxygen,[37] and was typically 0.064 ± 0.005 cm^2.

Preparation of the aptamer-modified electrodes. Clean electrodes were washed in water and kept in EtOH for 30 min prior modification. Cysteamine SAMs were formed by covering the electrode surface with a 10 μL drop of a 20 mM cysteamine solution for 2 h and keeping it under the lid. The

cysteamine-modified electrodes were rinsed in PBS. Thiolated aptamer samples were allowed to react with 0.5 mM TCEP for 1 h in order to reduce the disulfide bonds and then diluted with PBS to their final concentration of 10 μM. After that, a 10 μL drop of the aptamer solution was placed on the top of the cysteamine-modified electrode and left for 30 min at rt under the lid. The modified electrodes were then again carefully washed with PBS and stored in it at least for 15 min before use. All MB-containing solutions and MB-aptamer-modified electrodes were kept in dark.

Instrumentation and procedure. Cyclic voltammetry (CV) measurements were performed in a standard three-electrode cell connected to the potentiostat AUTOLAB PGSTAT 30 (Eco Chemie B.V., Utrecht, the Netherlands) equipped with a NOVA 1.10 software, with a gold working electrode; the counter electrode was a Pt wire, and an Ag/AgCl (3 M KCl) was the reference electrode (Metrohm, Denmark). In stability assessment, the MB redox CV signal recorded with the MB-aptamer-modified electrodes was followed as a function of time, and the modified electrodes were kept in 20 mM PBS, pH 7.4, at 4°C, between measurements. In the chronoamperometric measurements the working electrode fitted into a customized Teflon holder was inserted into a flow-through wall-jet electrochemical cell with an Ag/AgCl (0.1 M KCl) reference and Pt wire auxiliary electrodes. PBS, pH 7.4, and PBS containing 10% serum from new born fetal calf, pH 7.4, were used as working solutions, pumped through the electrochemical cell by the Gilson peristaltic pump (Gilson Minipuls 3, Villiers-le-Bel, France). The reproducibility of the data was verified by measurements with at least four equivalently prepared electrodes. Experiments were performed at 22 ± 1 °C.

RESULTS AND DISCUSSION

Characterization of the surface state of the aptamer and its binding properties

To determine the aptamer surface coverage and correlate it with the surface state/binding ability of the aptamer, the MB- and alkanethiol-modified aptamer was immobilized on the electrode surface and interrogated in the reaction with dopamine. A pronounced redox signal from the MB label, at around -246 ± 40 mV could be followed in CVs recorded with the aptamer-modified electrode in blank PBS (**Figure 2**). The intensity of the CV peak currents was linearly proportional to the potential scan rate, designating the surface-confined process.[38] The peaks full width at half maximum, FWHM, of 92±9 mV was larger than the expected for a $2e^-$ transfer reaction of MB[39] (FWHM=90.6/*n* mV), [40]being more consistent with a $1e^-$ transfer reaction (and the impeded protonation/transfer of the second electron).[41] To correlate dopamine ligand binding properties and

the surface state of the aptamer, the aptamer surface coverage (Γ_{RNA}) was calculated according to the equation $\Gamma_{RNA}=Q/nFA$. Here, n is the number of electrons transferred, F is the Faraday constant, A is the electrochemically determined surface area of the gold electrodes, and Q is the amount of electricity consumed in the redox reaction and determined by integrating the oxidation/reduction CV peaks of MB (**Figure 2**). Taking into account $1e^-$ involved in the redox reaction of MB under our experimental conditions (electrochemically determined, see ESI for more details),[42] the aptamer surface coverage was estimated to be 6.6 ± 0.2 pmol cm^{-2}, which is consistent with that previously found for a monolayer of electrostatically bound aptamer.[27]

It was earlier shown that the aptamer surface coverage essentially affected the dopamine binding ability of the aptamer, high surface densities of the aptamer causing steric hindrance for the binding of the analyte and low densities leading to low binding capacity.[27] Despite using a quite similar immobilization conditions optimized in our previous work[27], the Γ_{RNA} of 6.6 pmol cm^{-2} exceeds the optimal 3.5 ± 0.3 pmol cm^{-2} surface coverage of electrostatically bound RNA aptamer lying flat on the electrode surface. The higher surface coverage can be attributed to the competitive binding of the C6 alkanethiol linker to the electrode surface, by this replacing a part of the electrode-bound cysteamine molecules. This higher surface coverage should then result in the upright surface orientation of RNA strands, which, being tethered to the electrode through the linker, can partially sacrifice an electrostatic binding mode and extend themselves more in solution, and thus occupy less surface space. The Γ_{RNA} obtained here is about 77% of that reported for a compact monolayer of dsDNA of a ca. 35 Å in the cross-section diameter standing normal to the surface (8.6 pmol cm^{-2})[43] and approximately 44% of that reported for flexible polythymine ssDNA (15.4 pmol cm^{-2}).[44] According to[45], that corresponds to a mean neighbor strand separation of ~ 5 nm, which is generally sufficient for avoiding overcrowding and accompanying it steric hindrance of the neighboring oligonucleotides in specific biorecognition and binding of dopamine. [27]

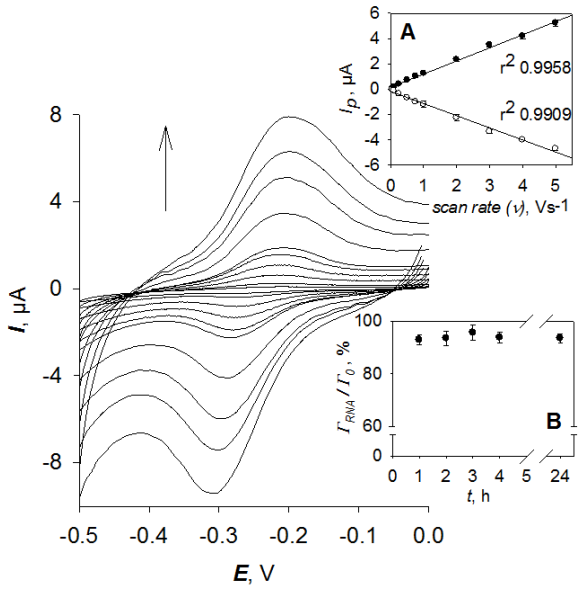

Figure 2. Representative CVs recorded with the MB-labeled aptamer-modified gold electrode in N_2-saturated 20 mM PBS, pH 7.4, potential scan rate: 0.05, 0.1, 0.25, 0.5, 0.75, 1, 2, 3, 4, and 5 V s^{-1} (the arrow designates the increasing scan rate). *Inset*: (**A**) Dependence of the anodic (I_{pa}) and cathodic (I_{pc}) peak intensities on the potential scan rate; and (**B**) variation of the normalized aptamer surface coverage Γ_{RNA} with time, Γ_0 is the aptamer surface coverage at time t=0.

The electron transfer (ET) rate constant for the redox reaction of MB estimated according to the Laviron theory was 19 ± 2 s^{-1}, which was close to the values obtained on mercaptopropionic acid SAMs (10-30 s^{-1}).[46] Despite the MB-terminal modification of the aptamer (**Figure 1B**, the top region of the aptamer), MB electrochemistry exhibited the features of the adsorbed state, MB species not diffusing in the electric double layer (EDL) as was earlier shown for MB-labeled ssDNA.[44,47] That might be expected, if the aptamer is still to a certain extent electrostatically attracted to the positively charged cysteamine co-adsorbate, used here to inhibit nonspecific binding and electrode reactions of the competitive catecholamines (see ESI, **Figures** S6-S8).

Stability of the aptamer binding to the electrode is of a paramount importance for practical applications in physiological fluids and reusable operation of the aptasensor, and it was much improved compared to the previous aptasensor design based solely on electrostatic interactions:[24] 93% of the initial surface coverage (Γ_0) was maintained within 24 h of the electrode storage (**Figure 2**, inset B). The first hour decrease in the Γ_{RNA} could be attributed to the loss of weakly/non-specifically bound aptamer molecules.

Therewith, the alkanethiol-tethered aptamer conserved its ability to selectively bind dopamine, and a well-defined redox signals stemming from dopamine appeared at around +194 ± 6 mV in

dopamine-containing solutions. Consistent with previous reports,[36] for dopamine concentrations below 5 μM the dopamine anodic peak intensity (I_{pa}) increased linearly with the potential scan rate (**Figure S1,** inset), designating a surface-confined ET reaction.

Dopamine binding by MB-labeled and unlabeled aptamers

Chronoamperometric analysis of dopamine in serum and sensor regeneration experiments were further performed by the flow-injection analysis (FIA), providing conditions for facilitated injection and removal of dopamine in the electrochemical system; it was used as a first approximation to the dopamine delivery and metabolism in living systems. The aptamer-modified gold electrodes were incorporated into a flow-through wall-jet electrochemical cell (**Figure 1**). We addressed (i) the ability of the aptamer to specifically recognize dopamine, (ii) sensor re-usability in a flow system, and (iii) kinetics of the affinity interactions between the aptamer and dopamine. The stability of the aptamer on electrodes was confirmed with the MB-labeled RNA sequence, and then the dopamine binding properties that could be affected by the presence of the MB label were studied both with the MB-labeled and label-free RNA aptamer sequences. Though the aptamer 3´ terminal labeling with a MB tag should not interfere with its binding properties in solution (the 3´ terminus of the aptamer is not directly involved in binding),[26] it might affect the surface reaction at the level of electrostatic interactions.[47]

A typical FIA current response to injections of 0.1 - 1 μM dopamine is shown in **Figure 3**. The amperometric responses of the MB-labeled and unlabeled aptamers to dopamine (**Figure 3,** inset) did not significantly differ and were similar with an inter-electrode precision (RSD) of 7%, under optimized experimental conditions (a flow rate of 0.8 mL min^{-1} and injection volumes of 300 μL) that were selected to avoid an excessive dispersion of the sample in the flow, provide mass transfer rates/times sufficient for dopamine interactions with the aptamer, and ensure a good operational stability of the sensor (**Figure S2** and **S3**, ESI, for more details).

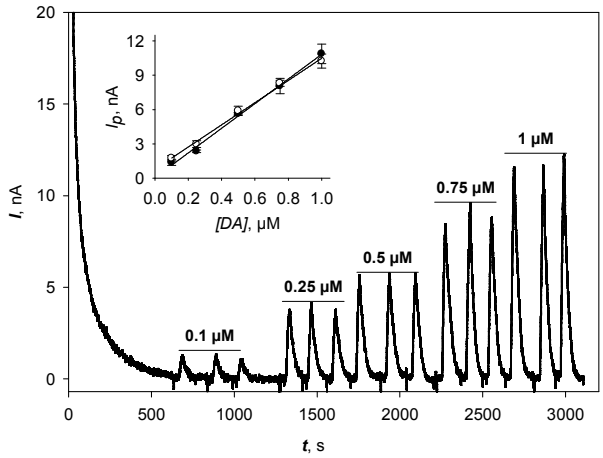

Figure 3. Representative FIA sensogram recorded with the aptamer-modified electrode upon successive injections of dopamine. *Inset*: Concentration dependence of the dopamine oxidation signal recorded with electrodes modified with (black circles) unlabeled and (white circles) MB-labeled aptamers (3 independent electrodes). Other conditions: 20 mM PBS, pH 7.4, as a carrier solution, 0.8 mL min^{-1} flow rate, E_d = +0.185 V *vs* Ag/AgCl (0.1 M KCl), at which dopamine oxidation currents are maximal (ESI, Figure S1), and 300 µL injection volume.

It can be seen in **Figure 3** that after each cycle of dopamine injection and oxidation, oxidized dopamine is released from the aptamer-modified surface, and by that restores the dopamine binding ability of the aptamer, which makes the biosensor re-usable. The aptamer itself was selected to be specific exclusively for the reduced form of dopamine[26], and that allows this natural and simple protocol of the aptasensor regeneration. If the oxidized dopamine molecules were still aptamer-bound, then, after the decay of the oxidation signal in the dopamine-free solutions, further reproducible binding and oxidation of dopamine from freshly injected samples could not be observed. This is indeed a crucial parameter for *in vivo* operation of the aptasensor.

The temporal response of the aptamer-modified electrode towards dopamine determined in the FIA system was ~ 1 s based on the time needed for 0.1 µM bolus of dopamine to enter the cell chamber, reach the electrode surface and start responding (NB: note that in the case of the immediate exposure of the aptamer-modified electrodes to dopamine this time will be reduced since it will include only the dopamine binding step). This temporal resolution approaches the requirements for *in vivo* measurements, where dopamine release occurs over a time range from 0.2 to less than 5 s.[5] The maximum peak response was obtained within ~7 s at a flow rate of 0.8 mL min^{-1}, representing the time necessary for the entire sample bolus to pass by the electrode surface. The sensitivity of analysis determined from the slope of the inset plots in **Figure 3** was 128 ± 10 nA μM^{-1} cm^{-2}, with a dopamine limit of detection (LOD) of 0.087 and 0.082 µM for MB-labeled and unlabeled

aptasensors, respectively. The LOD was calculated as three times the standard deviation of the blank response (σ) divided by the slope of the calibration curve (*i.e.* the LOD= 3σ/m). This result evidences that the MB redox label did not significantly affect the aptamer–DA binding affinity and, therefore, further analysis was performed with the unlabeled aptamer sequence, not the least to avoid the expensive step of RNA labeling.

Selectivity and stability of the aptasensor

One of the major problems encountered for *in vivo* monitoring of dopamine is the interference from catecholamines that have oxidation potentials overlapping with that of dopamine. The performance of the developed aptasensor in the selective electroanalysis of dopamine was assessed in the presence of such structurally related NTs as norepinephrine (NE), levodopa (L-DOPA), and catechol. Voltammetric responses from those NTs were impeded at the aptamer-modified electrode, which allowed the essential peak separation between dopamine signal (E_{pa} of 109 ± 11 mV) and other NTs (E_{pa} of at least 196 ± 13 mV) and discrimination between dopamine and interfering NTs (**Figure 4A**). The dopamine faradaic signal dominating over NT interferents' ones suggests that specific recognition and binding of dopamine by the aptamer favors the ET reaction between dopamine and the electrode, in contrast to those of NTs, at the same concentration levels. Interestingly, catechol, not bearing the positively charged amine group, produced the oxidation signal superior to other catecholamines, though still much lower than that from dopamine (**Figure 4**), evidencing a large role of electrostatic interactions in interfacial modulation of the aptamer specificity.

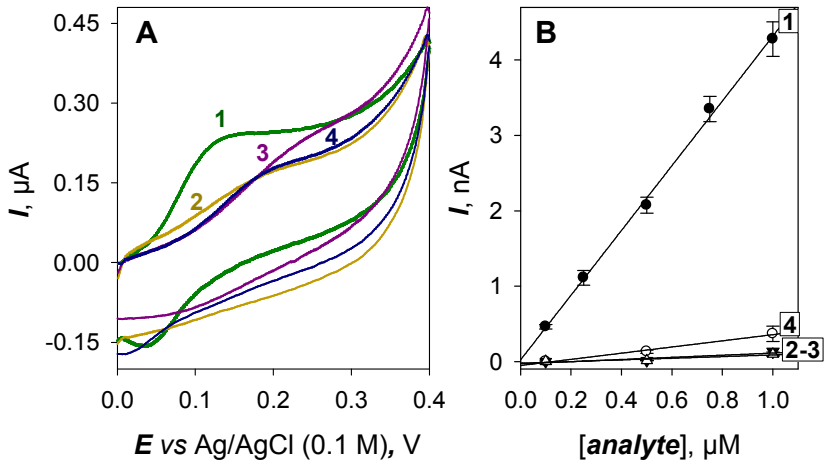

Figure 4. **A)** Representative CVs recorded with the aptamer-modified electrode in the FIA electrochemical cell in solutions of 6 μM (1) dopamine, (2) norepinephrine, (3) levodopa, and (4) catechol recorded potential scan rate 100 mV s^{-1}. **B)** Response of the aptamer-modified electrode to (1) dopamine and related

neurotransmitters: (2) norepinephrine, (3) levodopa and (4) catechol. Conditions: 20 mM PBS, pH 7.4, flow rate 0.8 mL min^{-1}, E_d +0.08 V *vs* Ag/AgCl (0.1 M KCl) and injection volume of 300 µL.

In control experiments performed with a dopamine-nonspecific DNA sequence instead of the RNA aptamer; both the sensitivity and specificity of the sensor were strongly compromised (ESI, **Figure S9**). In contrast to the data shown in **Figure 4A**, no selective binding and oxidation of dopamine could be followed with an arbitrary DNA sequence (ESI, **Figure S9A**), consistent with our previous results with mutated RNA aptamer and arbitrary DNA sequences.[24] This confirms that dopamine detection is due to specific binding of dopamine by the aptamer, though a minor response of the DNA-modified electrodes to higher concentrations of dopamine (the intensity of the oxidation signal from 1 µM dopamine not exceeding the response of the aptasensor for 0.1 µM dopamine), due to its electrostatic binding to arbitrary DNA, was not excluded (**Figure S9B**)

Specificity of electroanalysis was further tested by chronoamperometry at +80 mV in a flow-injection mode, when dopamine, NE, L-DOPA, and catechol were injected into the continuous flow stream of the buffer solution. As can be seen (**Figure 4B**), the detection potential, E_d, of +80 mV is sufficiently high for a pronounced response from dopamine in the concentration range of interest (0.1—1 µM), and sufficiently low to ensure negligible responses from the structurally related NTs (**Table S1**). The dopamine current signal varied linearly with the dopamine concentration, and dopamine could be analyzed with a sensitivity of 67 ± 1 nA μM^{-1} cm^{-2} and an LOD of 62 nM. Thus, the immobilization of the aptamer on the electrode surface through the alkanethiol linker did not interfere with the specificity and sensitivity of electroanalysis and approached that earlier reported for the dopamine aptamer electrostatically bound to the electrode surface (62 ± 2 nA μM^{-1} cm^{-2}).[24]

Therewith, the operational stability of the aptasensor operation was much improved. During 1 h operation of the aptamer-modified electrodes in the flow-injection system, with repetitive injections of 0.5 µM dopamine, no significant loss in the dopamine oxidation signal has been observed. (**Figure S4**). The relative standard deviation (RSD) for the peak intensities (n=20 injections) was less than 10%, demonstrating the stability of the aptamer immobilization, reversibility of the binding interactions and reliability of the aptasensor response. Overall these features indicate that the aptasensor can be used in real-time experiments and applicable for continuous specific monitoring of dopamine, which is particularly important for *in vivo* applications, where the electrodes are typically used for prolonged times in order to measure neurotransmission in behavioral or pharmacological experiments.

Kinetics of binding and ligand binding affinities of between dopamine and the RNA aptamer

Kinetic analysis of ligand-binding interactions in the dopamine-aptamer complex could provide more information about interfacial properties of the aptamer, modulated by the structure of the interface. First, the kinetics of binding of dopamine to the RNA aptamer were studied as a function of dopamine concentration. As is seen from the chronoamperogram (**Figure 5**), the formation of the dopamine-RNA complex at the electrode surface starts immediately after injection of dopamine, and the oxidation current increases exponentially, from zero to the maximal value corresponding to the maximal surface concentration of the dopamine-RNA complex, [dopamine— RNA aptamer]$_{max}$. It is important, that even under the saturation concentration conditions the dopamine signal is very reproducible (RSD 3%) and returns to the original background after the washing-off step; such behavior confirms a full reversibility of the biorecognition process and that the aptasensor can be regenerated under hydrodynamic conditions without extra treatment. This is particularly remarkable because at high dopamine concentrations the products of dopamine oxidation (i.e. leucodopaminechrome and melanin-similar compounds, **Figure S5**) have a tendency to foul the electrode surface;[48] thus, the aptasensor resistance to fouling allows prolonged and reliable electrochemical analysis.

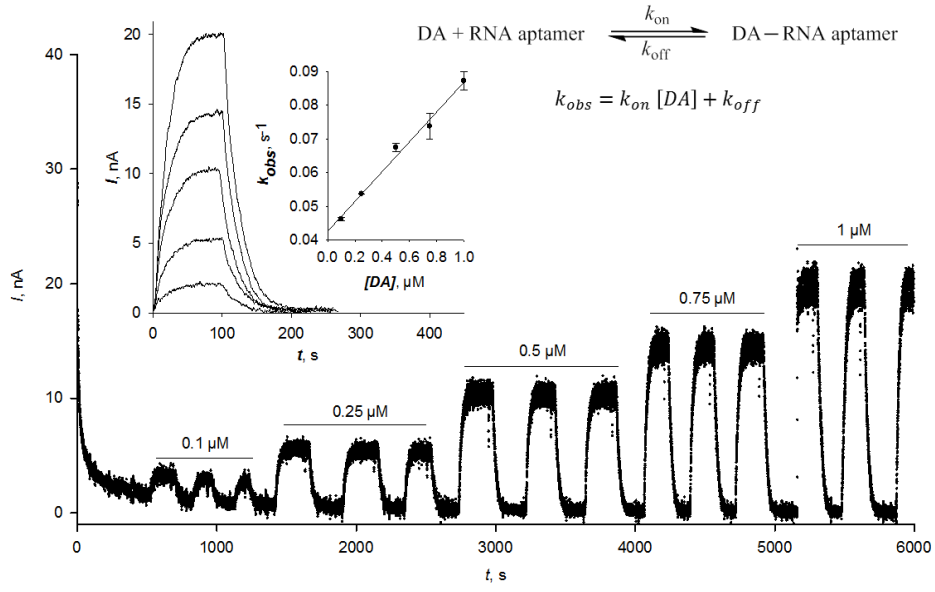

Figure 5. Representative flow-injection amperometric response of the aptamer modified electrode to three consecutive injections of similar concentrations of dopamine. **Inset**: The observed rate constants (k_{obs}) plotted against dopamine concentration (0.1, 0.25, 0.5, 0.75, and 1 μM dopamine, from the bottom to the top). Other conditions: detection potential + 185 mV *vs* Ag/AgCl (0.1 M KCl), 20 mM PBS, pH 7.4, flow rate of 0.8 mL min^{-1} and a 1.3 mL injection volume. [DA] is the concentration of dopamine.

For processes associated with surface binding, the reaction between the ligand and the immobilized biorecognition unit needs some time to reach the equilibrium after the analyzed ligand (in our case, dopamine) is injected in the system, and the time-dependent response does not instantly increase, but is slowed down, with a rounded characteristic shape of the response curve[49] consistent with amperometric response profiles in **Figure 5**.

Under the assumptions of a single binding site per one aptamer molecule and reversible dopamine binding, the experimental plots from **Figure 5** can be fitted to the first-order binding rate law[50,51] given by the mono-exponential Eq. (1):[52]

$$\frac{[DA—RNA\ aptamer]_t}{[DA—RNA\ aptamer]_{max}} = 1 - e^{-k_{obs}\,t} \qquad (1)$$

where [DA—RNA aptamer]$_t$ is the amount of complex at the considered time, [DA—RNA aptamer]$_{max}$ is the maximal concentration of the dopamine-aptamer complex corresponding to the current plateau value, and k_{obs} is the observed rate constant for each dopamine concentration. The apparent association and dissociation rate constants (k_{on} and k_{off}) are then calculated by plotting the k_{obs} values against the concentration of dopamine. The resulting plot (**Figure 5,** inset) shows a linear dependence of the rate constant on the dopamine concentration, which confirms the hypothesized first order binding kinetics. The k_{on} value extracted from the slope of the regression line gives us general information on the complex stability and how strong are the affinity interactions in the formed dopamine—RNA aptamer complex. The slope yields the k_{on} of (4.4 ± 0.3) × 10^4 $M^{-1}s^{-1}$ at 23 °C, which is comparable with the association rate constant for binding of PSA to the monoclonal antibody (4.1 x 10^4 $M^{-1}s^{-1}$).[53] The k_{off} of (4.3 ± 0.1) ×10^{-3} s^{-1} was obtained from the intercept of the linear regression line with the Y-axis and therefore, the equilibrium dissociation constant (K_D, defined as k_{off}/k_{on}) was 1.03 ± 0.09 μM. This value approaches 1.6 μM previously reported for the formation of the dopamine—RNA aptamer complex in solution (obtained by equilibrium filtration)[26] and indicates that immobilization of the aptamer did not significantly affect its binding properties. Along with that, due to the surface-modulated electrostatic interactions, affinity of other NTs for the aptamer was depressed compared to that shown in solution, where norepinephrine, L-DOPA and catechol were able to elute 58, 30 and 23% of the dopamine-agarose bound aptamer.[26]

If one compares the K_D values obtained in solution to those extracted from the current response-analyte concentration dependencies fitted to the Langmuir isotherm,[27,54] the latter yield lower values

of dissociation constants, which reflects that those are apparent dissociation constants ($K_{D,apparent}$) that depend not on the true affinity of analytes for their aptamers, usually measured under equilibrium conditions, but on the analyte concentration evaluated by dynamic electrochemical methods.[55] This issue may also lead to discrepancies between the reported limits of detection and $K_{D,apparent}$, such as in case of the uPA-specific fluorinated RNA aptamer ($K_{D,apparent}$ of 2.27 nM and the linear detection range of 1 pM – 1nM)[54] or the tobramycin binding RNA aptamer ($K_{D,apparent}$ of 16 μM and the linear detection range of 2.6 – 12.5 μM).[56]

Finally, the equilibrium binding energy (ΔG) of dopamine to the aptamer was estimated from $\Delta G = -RT \ln(1/K_D)$[57] as –8.135 kcal mol^{-1}, which agrees with the values obtained for other switchable aptamers, such as the theophylline binding one (–8.86 kcal mol^{-1}).[58] This indicates that even though the aptamer has to undergo certain conformational changes for dopamine binding, this step is thermodynamically favorable, and the dopamine binding pocket is stabilized after the formation of the dopamine–aptamer complex.

Electroanalysis of dopamine in serum

Finally, the RNA aptasensor was tested under experimental conditions mimicking those in biological systems. Amperometric analysis in the FIA system was performed in solutions containing 10% of fetal calf serum spiked with increasing concentrations of dopamine (**Figure 6**). Although serum contains a variety of blood proteins/nucleases and other biomolecules, the sensitivity (72 ± 4 nA μM^{-1} cm^{-2}) obtained from the calibrations plots (**Figure 6,** inset A) was comparable to that observed in PBS (67 ± 1 nA μM^{-1} cm^{-2}). Thus, in a short time scale the recorded signal appeared to be insensitive to non-specific adsorption of serum components. Quite similar data were previously obtained with RNA[42,54] and DNA[59] aptamer sensors, which sensing, at negative charges of the electrode surface, was insensitive to serum interference.

However, upon exposure to serum for prolonged times, exceeding 10 min, an ~ 20% oxidation signal decrease was observed, with a sensitivity decreasing to 51 ± 2 nA μM^{-1} cm^{-2} (**Figure 6** inset B), which can be attributed to a partial passivation of the electrode surface by serum proteins.[60,61] Nonetheless, the aptasensor preserved its response in dopamine binding and oxidation in a quite reproducible manner, which after 20 h of exposure to serum stayed at the same level (**Figures 6B and S10**), meaning that the signal generation mechanism remained effective also after signal original inhibition in the complex physiological matrix. Another important observation relates to the issues with RNA instability against chemical and enzymatic digestion: it follows from our results

that RNA immobilization on the electrode surface improves the RNA aptamer stability without altering its ability to bind its specific target.

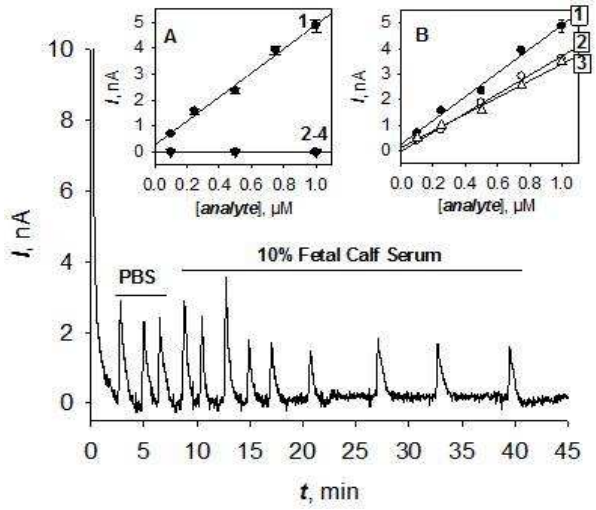

Figure 6. Representative amperometric response of the aptamer-modified electrode placed in the flow-injection wall-jet cell to consecutive injections of 0.5 μM DA in 20 mM PBS, pH 7.4, and PBS containing 10% of serum. Inset (A): calibration curves of (1) dopamine, (2) NE, (3) catechol, and (4) L-DOPA obtained in PBS/10% serum. Inset (B): dependence of the oxidation peak current on dopamine concentration obtained from (1) initial dopamine signals in PBS/10% serum and after (2) 30 min and (3) 20 hours exposure to serum. Detection potential + 80 mV *vs* Ag/AgCl (0.1 M KCl), injection volume 300 μL and a flow rate 0.8 mL min^{-1}.

The aptasensor is thus compatible with biological samples, approaching the requirements of the temporal resolution and sensitivity/LOD adequate for its application for real-time monitoring of dopamine in biological media. Importantly, specific analysis of dopamine by the aptamer-modified electrodes currently seems to be the simplest and most reliable of the hitherto suggested approaches (**Table S2**) as well as the most applicable for *in vivo* analysis. Recently, a colorimetric sensor based on Au@Ag nanorods that can be used for analysis of dopamine in biological samples has been developed[62] and the sensitivity of detection was significantly improved to 0.006 pM, when nanorods were modified with the aptamer and combined with Raman scattering detection.[63] Encouraging results in terms of sensitivity and selectivity have been also reported with fluorescein and nile blue-functionalized gold nanoparticles[64] and water soluble Si nanoparticles,[65] as well as with quantum dots as electrochemiluminescence emitters, leading to the detection limit of 26 pM and successfully used in cerebrospinal fluid samples.[66] Another reasonable alternative is a bioaffinity sensor based on surface plasmon resonance using a dopamine receptor as a biorecognition unit.[21] However, all these reported approaches are hardly applicable for real-time *in vivo* monitoring of dopamine. Other reported sensing schemes for real sample analysis generally

report only interference from ascorbic acid and uric acid and, thus, the possibility of specific analysis of dopamine by those assays in the presence of structurally related NTs remains unclear.

CONCLUSIONS

A label-free electrochemical sensor for dopamine analysis, exploiting an alkanethiol-conjugated dopamine RNA aptamer tethered to the cysetamine-modified gold electrodes through the thiol linkage, demonstrates a quite fast response in the FIA system (< 1 s, accounting also for dopamine transportation to the electrodes), appropriate for *in vivo* sensing sensitivity (67 ± 1 nA μM^{-1} cm^{-2}), the limit of detection within the physiologically important concentration range (10 nM—1 μM),[5] and stability suitable for continuous use in flow systems with serum samples. The improved selectivity of dopamine electroanalysis in the presence of the competitive NT catecholamines is also provided by the modulation of the aptamer and electrode surface charges by the positively charged cysteamine SAM. Therewith, the dopamine-RNA aptamer binding is not affected by the aptamer surface immobilization, and the evaluated dissociation constant K_D of 1.03 ± 0.09 μM approaches 1.6 μM shown in solution. Given the simplicity of the design and demonstrated possibility of the RNA aptasensor operation in serum, the developed approach can be used to produce miniaturized sensors that can be implanted in living organisms and used to monitor dopamine-related biological processes with high spatiotemporal resolution and chemical specificity. In particular, the dopamine aptasensor can productively contribute to the development of complex *in vivo* electroanalytical platforms for diagnostics and studies of mechanisms of neurodegenerative diseases,[32-35] also by providing reliable and specific methodology for analysis of dopamine levels in patients' blood plasma and serum that will be supplementary to the existing clinical research.[4]

ACKNOWLEDGEMENTS

The work was supported by the Danish National Research Foundation (DNRF) through their support to the CDNA, grant number DNRF81. IÁM thanks the FICYT and the 7th WP of the European Union, Marie Curie Actions, for the post-doctoral grant ACA14-22.

SUPPORTING INFORMATION

Additional details on kinetic calculations and reaction schemes; additional CV and chronoamperometric data, and data on operational stability of the aptasensor; tables referring the sensitivity and selectivity of the existing dopamine sensors.

REFERENCES

(1) Kalia, L. V.; Lang, A. E. *Lancet* **1996**, *386*, 896-912.
(2) Usiello, A.; Baik, J.-H.; Rouge-Pont, F.; Picetti, R.; Dierich, A.; LeMeur, M.; Piazza, P. V.; Borrelli, E. *Nature* **2000**, *408*, 199-203.
(3) Hashizume, K.; Yamatodani, A.; Ogihara, T. *Hypertens. Res.* **1995**, *18*, Suppl. I: S205-S207.
(4) Riggin, R. M.; Alcorn, R. L.; Kissinger, P. T. *Clin. Chem.* **1976**, *22*, 782-784.
(5) Michael, A. C.; Borland, L. M.; Robinson, D. L.; Wightman, R. M. In *Electrochemical Methods for Neuroscience*, Michael, A. C.; Borland, L. M., Eds.; CRC Press: Boca Raton 2007.
(6) Saylor, R. A.; Lunte, S. M. *J. Chromatogr. A* **2015**, *1382*, 48-64.
(7) Watson, C. J.; Venton, B. J.; Kennedy, R. T. *Anal. Chem.* **2006**, *78*, 1391-1399.
(8) Robinson, D. L.; Hermans, A.; Seipel, A. T.; Wightman, R. M. *Chem. Rev.* **2008**, *108*, 2554-2584.
(9) Wightman, R. M.; Jankowski, J. A.; Kennedy, R. T.; Kawagoe, K. T.; Schroeder, T. J.; Leszczyszyn, D. J.; Near, J. A.; Diliberto, E. J.; Viveros, O. H. *Proc. Nail. Acad. Sci. USA* **1991**, *88*, 10754-10758.
(10) Baur, J. E.; Kristensen, E. W.; May, L. J.; Wiedemann, D. J.; Wightman, R. M. *Anal. Chem.* **1988**, *60*, 1268-1272.
(11) Mosharov, E. V.; Sulzer, D. *Nature Methods* **2005**, *2*, 651-658.
(12) Cahill, P. S.; Walker, Q. D.; Finnegan, J. M.; Mickelson, G. E.; Travis, E. R.; Wightman, R. M. *Anal. Chem.* **1996**, *68*, 3180-3186.
(13) Troyer, K. P.; Wightman, R. M. *J Biol. Chem.* **2002**, *277*, 29101-29107.
(14) Hochstetler, S. E.; Puopolo, M.; Gustincich, S.; Raviola, E.; Wightman, R. M. *Anal. Chem.* **2000**, *72*, 489-496.
(15) Hermans, A.; Keithley, R. B.; Kita, J. M.; Sombers, L. A.; Wightman, R. M. *Anal. Chem.* **2008**, *80*, 4040-4048.
(16) Makos, M. A.; Han, K.-A.; Heien, M. L.; Ewing, A. G. *ACS Chem. Neurosci.* **2010**, *1*, 74-83.
(17) Sun, M.; Kaplan, S. V.; Gehringer, R. C.; Limbocker, R. A.; Johnson, M. A. *Anal. Chem.* **2014**, *86*, 4151-4156.
(18) Spegel, C.; Heiskanen, A.; Acklid, J.; Wolff, A.; Taboryski, R.; Emneus, J.; Ruzgas, T. *Electroanalysis* **2007**, *19*, 263-271.
(19) Jackowska, K.; Krysinski, P. *Anal. Bioanal. Chem.* **2013**, *405*, 3753-3771.
(20) Baur, J. E.; Kristensen, E. W.; May, L. J. M.; Wiedemann, D. J.; Wightman, R. M. *Anal. Chem.* **1988**, *60*, 1268-1272.
(21) Kumbhat, S.; Shankaran, D. R.; Kim, S. J.; Gobi, K. V.; Joshi, V.; Miura, N. *Biosens. Bioelectron.* **2007**, *23*, 421-427.
(22) Xiang, L.; Lin, Y.; Yu, P.; Su, L.; Mao, L. *Electrochim. Acta* **2007**, *52*, 4144-4152.
(23) Lin, Y.; Zhang, Z.; Zhao, L.; Wang, X.; Yu, P.; Su, L.; Mao, L. *Biosens. Bioelectron.* **2010**, *25*, 1350-1355.
(24) Farjami, E.; Campos, R.; Nielsen, J.; Gothelf, K.; Kjems, J.; Ferapontova, E. E. *Anal. Chem.* **2013**, *85*, 121-128.
(25) Ferapontova, E. E.; Gothelf, K. V. *Curr. Org. Chem.* **2011**, *15*, 498-505.

(26) Mannironi, C.; Di Nardo, A.; Fruscoloni, P.; Tocchini-Valentini, G. P. *Biochemistry* **1997**, *36*, 9726-9734.
(27) Álvarez-Martos, I.; Campos, R.; Ferapontova, E. E. *Analyst* **2015**, *140*, 4089-4096.
(28) Ferapontova, E.; Gothelf, K. V. *Langmuir* **2009**, *25*, 4279-4283.
(29) Ferapontova, E. E.; Olsen, E. M.; Gothelf, K. V. *J. Am. Chem. Soc.* **2008**, *130*, 4256-4258.
(30) Waxman, E. A.; Giasson, B. I. *Biochim. Biophys.Acta* **2009**, *1792*, 616-624.
(31) Cookson, M. R. *Mol. Neurodegen.* **2009**, *4*, 9.
(32) Vestergaard, M. d.; Kerman, K.; Saito, M.; Nagatani, N.; Takamura, Y.; Tamiya, E. *J. Am. Chem. Soc.* **2005**, *127*, 11892-11893.
(33) Lopes, P.; Dyrnesli, H.; Lorenzen, N.; Otzen, D.; Ferapontova, E. E. *Analyst* **2014**, *139*, 749-756.
(34) Lopes, P.; Ferapontova, E. E. *Monatsh. Chem.* **2015**, *146* 781-786.
(35) Lopes, P.; Xu, M.; Zhang, M.; Zhou, T.; Yang, Y.; Wang, C.; Ferapontova, E. E. *Nanoscale* **2014**, *6*, 7853-7857.
(36) Farjami, E.; Campos, R.; Nielsen, J. S.; Gothelf, K. V.; Kjems, J.; Ferapontova, E. E. *Anal. Chem.* **2012**, *85*, 121-128.
(37) Hoogvliet, J. C.; Dijksma, M.; Kamp, B.; van Bennekom, W. P. *Anal. Chem.* **2000**, *72*, 2016-2021.
(38) Bard, A. J.; Faulkner, L. R. *Electrochemical Methods - Fundamental and Applications*, 2nd ed.; Wiley: New York, 2001.
(39) Ferapontova, E. E. *Curr. Anal. Chem.* **2011**, *7*, 51-62.
(40) Laviron, E. *J. Electroanal. Chem.* **1979**, *101*, 19-28.
(41) Campos, R.; Kotlyar, A.; Ferapontova, E. E. *Langmuir* **2014**, *30*, 11853-11857.
(42) Ferapontova, E. E.; Gothelf, K. V. *Electroanalysis* **2009**, *21*, 1261-1266.
(43) Hartwich, G.; Caruana, D. J.; de Lumley-Woodyear, T.; Wu, Y.; Campbell, C. N.; Heller, A. *J. Am. Chem. Soc.* **1999**, *121*, 10803-10812.
(44) Uzawa, T.; Cheng, R. R.; White, R. J.; Makarov, D. E.; Plaxco, K. W. *J. Am. Chem. Soc.* **2010**, *132*, 16120-16126.
(45) Watkins, H. M.; Simon, A. J.; Ricci, F.; Plaxco, K. W. *J. Am. Chem. Soc.* **2014**, *136*, 8923-8927.
(46) Benítez, G.; Vericat, C.; Tanco, S.; Lenicov, F. R.; Castez, M. F.; Vela, M. E.; Salvarezza, R. C. *Langmuir* **2004**, *20*, 5030-5037.
(47) Abi, A.; Ferapontova, E. E. *J. Am. Chem. Soc.* **2012**, *134*, 14499-14507.
(48) Harreither, W.; Trouillon, R.; Poulin, P.; Neri, W.; Ewing, A. G.; Safina, G. *Anal. Chem.* **2013**, *85*, 7447-7453.
(49) Jacobs, C. B.; Ivanov, I. N.; Nguyen, M. D.; Zestos, A. G.; Venton, B. J. *Anal. Chem.* **2014**, *86*, 5721-5727.
(50) Jucker, F. M.; Phillips, R. M.; McCallum, S. A.; Pardi, A. *Biochemistry* **2003**, *42*, 2560-2567.
(51) Challier, L.; Miranda-Castro, R.; Marchal, D.; Noël, V.; Mavré, F.; Limoges, B. *J. Am. Chem. Soc.* **2013**, *135*, 14215-14228.
(52) Goodrich, J. A.; Kugel, J. F. *Binding and Kinetics for Molecular Biologists*; Laboratory Press: Cold Spring Harbor, N.Y. , 2007.

(53) Kapil, M. A.; Herr, A. E. *Anal. Chem.* **2014**, *86*, 2601-2609.
(54) Jarczewska, M.; Kekedy-Nagy, L.; Nielsen, J. S.; Campos, R.; Kjems, J.; Malinowska, E.; Ferapontova, E. E. *Analyst* **2015**, *140*, 3794-3802.
(55) Esteban Fernández de Ávila, B.; Watkins, H. M.; Pingarrón, J. M.; Plaxco, K. W.; Palleschi, G.; Ricci, F. *Anal. Chem.* **2013**, *85*, 6593-6597.
(56) Schoukroun-Barnes, L. R.; Wagan, S.; White, R. J. *Anal. Chem.* **2014**, *86*, 1131-1137.
(57) Gilbert, S. D.; Stoddard, C. D.; Wise, S. J.; Batey, R. T. *J. Mol. Biol.* **2006**, *359*, 754-768.
(58) Wachsmuth, M.; Findeiß, S.; Weissheimer, N.; Stadler, P. F.; Mörl, M. *Nucleic Acids Res.* **2013**, *41*, 2541-2551.
(59) Xiao, Y.; Lubin, A. A.; Heeger, A. J.; Plaxco, K. W. *Angew. Chem.* **2005**, *117*, 5592-5595.
(60) Liu, J.; Wagan, S.; Dávila Morris, M.; Taylor, J.; White, R. J. *Anal. Chem.* **2014**, *86*, 11417-11424.
(61) Ferapontova, E. E.; Gothelf, K. V. *Langmuir* **2009**, *25*, 4279-4283.
(62) Liu, J.-M.; Wang, X.-X.; Cui, M.-L.; Lin, L.-P.; Jiang, S.-L.; Jiao, L.; Zhang, L.-H. *Sens. Actuat. B* **2013**, *176*, 97-102.
(63) Tang, L.; Li, S.; Han, F.; Liu, L.; Xu, L.; Ma, W.; Kuang, H.; Li, A.; Wang, L.; Xu, C. *Biosens. Bioelectron.* **2015**, *71*, 7-12.
(64) Zeng, Z.; Cui, B.; Wang, Y.; Sun, C.; Zhao, X.; Cui, H. *ACS Appl. Mater. Interfaces* **2015**, *7*, 16518-16524.
(65) Zhang, X.; Chen, X.; Kai, S.; Wang, H. Y.; Yang, J.; Wu, F. G.; Chen, Z. *Anal. Chem.* **2015**, *87*, 3360-3365.
(66) Zhang, L.; Cheng, Y.; Lei, J.; Liu, Y.; Hao, Q.; Ju, H. *Anal. Chem.* **2013**, *85*, 8001-8007.

FOR TOC ONLY

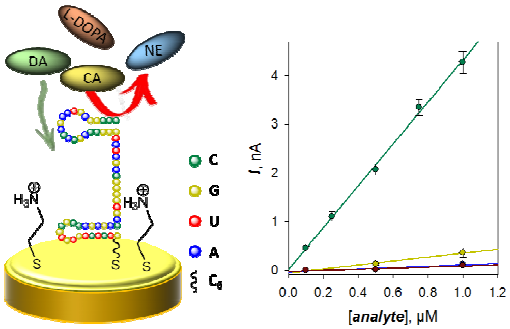
L-DOPA
DA
CA
NE
C
G
U
A
C_6
S
S
S
H_3N
H_3N
I, nA
0
1
2
3
4
0.0
0.2
0.4
0.6
0.8
1.0
1.2
[analyte], μM

BRIEFS

Physiologically relevant sub-micromolar analysis of dopamine in serum in the presence of competitive neurotransmitters including catechol, norepinephrine, and L-DOPA can be achieved with the RNA aptamer tethered to cysteamine-modified gold electrodes via the alkanethiol linker. The proposed biosensor design allows direct monitoring of dopamine levels in biological fluids in the presence of competitive NT, and thus may be applicable in biomedical research.